FACTA UNIVERSITATIS
Series: **Electronics and Energetics** Vol. 37, Nº 2, June 2024, pp. 355 - 368
https://doi.org/10.2298/FUEE2402355H

Original scientific paper

EXPERIMENTAL AND NUMERICAL ANALYSIS OF THE INFLUENCE OF THE CONTACT RESISTANCE IN A HIGH-POWER FUSE ON ITS TIME-CURRENT CHARACTERISTIC*

Ivan Hadzhiev, Dian Malamov, Nikolay Kolev, Iosko Balabozov, Ivan Yatchev

Technical University of Sofia - Plovdiv Branch, University of Plovdiv Paisii Hilendarski, Technical University of Sofia, Bulgaria

ORCID iDs:	Ivan Hadzhiev	https://orcid.org/0000-0003-2713-5186
	Dian Malamov	https://orcid.org/0000-0003-0782-497X
	Nikolay Kolev	N/A
	Iosko Balabozov	https://orcid.org/0000-0003-2011-6089
	Ivan Yatchev	https://orcid.org/0000-0001-6602-5102

Abstract. *This paper presents a study of thermal processes and time-current characteristics of a high-power low-voltage fuse at normal and increased contact resistance. Experimental and numerical studies have been performed. The experimental studies have been carried out by means of an experimental setup, especially developed for the purpose. Temperature measurement has been realised both by a contact thermometer and by a thermovision camera. The finite element method has been used in the numerical study. A computer model of the fuse has been developed in the software product COMSOL. The model reads the thermal processes in the fuse, as well as the heat transfer to the environment, which occurs by radiation and convection. Results about the influence of the contact resistance on the fuse heating and its time-current characteristic have been obtained. The obtained experimental and numerical results have been compared.*

Key words: *Contact resistance, high-power fuse, limiting current, thermal processes, time-current characteristic*

1. INTRODUCTION

Fusible fuses are among the most widely used protective electrical devices in industry and at home. Therefore, they have been subjected to a number of experimental and numerical studies. Paper [2] presents a study of the influence, exerted by the current higher harmonics on

Received November 27, 2023; revised January 31, 2024; accepted February 01, 2024
Corresponding author: Ivan Hadzhiev
Technical University of Sofia, Plovdiv Branch, Faculty of Electronics and Automation, Tsanko Dyustabanov 25, 4000 Plovdiv, Bulgaria
E-mail: hadzhiev_tu@abv.bg
*An earlier version of this paper was presented at the 16th International Conference on Applied Electromagnetics (ПЕС 2023), August 28 -30, 2023, in Niš, Serbia [1].

the power losses. Paper [3] goes further and discusses the influence of the harmonics and their frequency on the melting time of the fuse link, based on a model, developed in ANSYS. The effect of the current and the ambient temperature on the temperature distribution in a high-power fuse is described in [4]. A 3D model of a low voltage fusible fuse, developed by the finite element method, is presented in [5]. This model needs upgrading because of the deviations between the numerical and experimental results. Paper [6] suggests a new simulation model of fuses with high-breaking capacity and this model also needs improvement, to allow for taking into account the fuse temperature and the slow speed of the melting processes. The characteristics I2t of fuses for protecting semiconductors are considered in paper [7], and paper [8] studies the temperature distribution in a fast fuse for semiconductor protection by means of a developed model. Carried out again by means of purposefully developed computer models, a study of the thermal field in fuses for domestic application is described in [9].

Experimental and numerical studies of thermal processes in a high-power low-voltage fuse have been reported in [10]÷[14]. The numerical studies have been carried out by means of the finite element method and with the help of a developed by the authors computer model of the fuse in the software product COMSOL. Numerical results, concerning the electrical and thermal fields of the fuse at steady-state mode have been obtained. In [10] the model has been verified by comparing with experimental results about the fuse heating, obtained with the help of a purposefully developed experimental setup, while in [11] a thermovision camera has been used to study the fuse heating. Paper [12] presents numerical results, revealing the influence of the contact resistance on both the electric and the thermal field of the fuse at steady-state mode, and number [13] studies the influence of the cross-section of the connecting conductors in the fuse on its heating. In paper [14], the influence of external losses on the heating of the fuse with different lengths of connecting conductors is examined. Such losses can be generated by switching devices, power distribution blocks [15], and other devices connected in the fuse circuit.

Experimental and numerical studies of the time-current characteristics of the fuse within the limiting current region have been presented in a previous work of the authors. The research on the high-power low-voltage fuse has continued and this paper presents a study of the influence of the contact resistances on the time-current characteristics of the fuse. The experimental studies were performed by an experimental setup, developed on the purpose, and the numerical studies were carried out by means of a 3D computer model synthesized in a transient mode in COMSOL. The paper gives: a description of the construction of the studied fuse, experimental results about the influence of the contact resistance on the time-current characteristic and heating of the fuse, a mathematical model for solving the coupled electrical-thermal problem in a transient mode, the synthesis of a 3D computer model of the fuse and numerical results about the influence of the contact resistance on the time-current characteristic and the thermal processes in the fuse. Analysis was made and conclusions drawn up based on the obtained experimental and numerical results.

2. CONSTRUCTION OF THE STUDIED HIGH-POWER LOW-VOLTAGE FUSE

The subject of the study is a high-power low-voltage fuse with rated current of I_n=50 A, rated voltage U_n=500 VAC, short-circuit breaking capacity I_{cu}=120 kA and protective characteristic gG. This characteristic means that the fuse is a general purpose one and protects over the entire range from rated current to short-circuit breaking capacity. The photo of the studied fuse and its construction, developed in the COMSOL program, are shown in Fig. 1.

The cartridge is made of steatite, the covering plates, which close the cartridge, are aluminum. The contact knives and the fusible link are made of copper and the metallurgic effect is used. The contact knives are silver plated. Quartz sand is used as a fuse filler. The base and the connecting wires are made of copper. The insulation of the cables is Polyvinyl chloride (PVC).

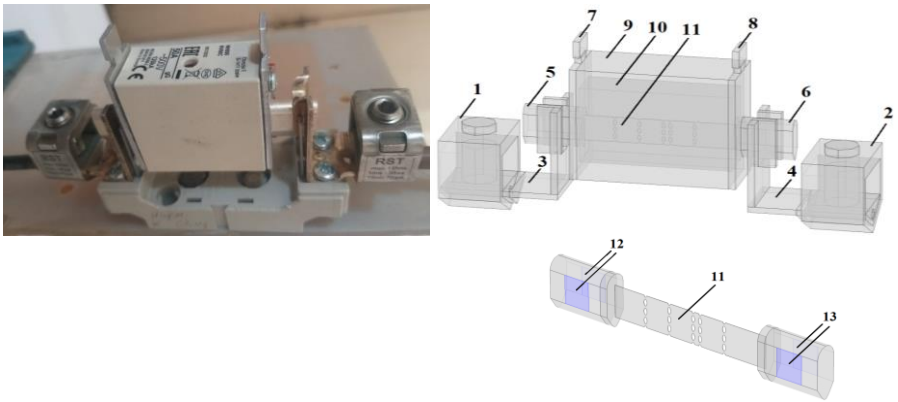

a) Photo of the studied fuse b) Computer model (the cables not shown)

Fig. 1 Construction of a high-power low-voltage fuse: 1, 2 – V-terminals; 3, 4 – base, on which the fuse is placed; 5, 6 – contact knives of the fuse; 7, 8 – covering plates, which close the cartridge; 9 – cartridge; 10 – fuse filler; 11 – fuse link; 12, 13 - apparent contact areas S_c of the contact connections between the contact knives and the base.

3. EXPERIMENTAL STUDY OF THE HIGH-POWER LOW-VOLTAGE FUSE

3.1. Electric circuit diagram of the experimental setup

Fig. 2 shows the diagram of the electric circuit of the developed for the purpose of studying the fuse heating experimental setup. The fuse temperature was measured by a thermovision camera and a contact thermometer. The current load and the actuation time were measured by a digital oscilloscope. Both the cross-sections and the lengths of the connecting cables were chosen in accordance with [16].

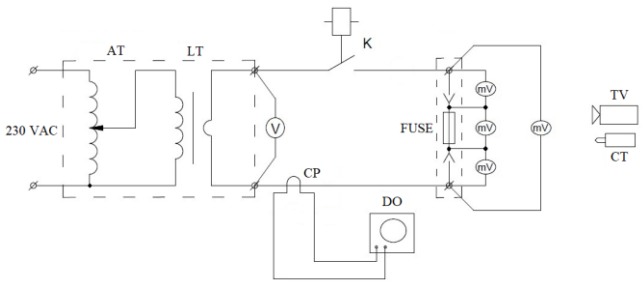

Fig. 2 Electric circuit diagram of the experimental setup: AT – autotransformer; LT – load transformer; V – voltmeter; K – contactor; mV – millivoltmeter; CP – current probe; DO – digital oscilloscope; TV – thermovision camera; CT – contact thermometer

3.2. Experimental results about the fuse heating at normal and increased resistances at a rated current load

Experimental studies were carried out on the heating of the fuses in a transient mode until reaching steady-state thermal mode under the rated current load of the fuse of I_n=50 A. The fuse temperature was measured in two points: on the cartridge and on its contact knife. Thirty (30) fuses were studied. Results were obtained about their heating at normal and increased resistances. The contact resistances were measured for new bases and fuses, and the increased resistances were accomplished by increase in the contact resistances between the fuse knives and the terminals of the base. The increased contact resistances are realized by placing thin plates of high electrical resistivity material between the fuse contact knife and the fuse base terminal. The averaged value of the normal contact resistance is R_{nc}=0.028 mΩ, and the averaged value of the uncreased contact resistance is R_{ic}=7.355 mΩ. Figs. 3÷5 present part of the results, obtained by a thermovision camera in a transient mode at a coefficient of radiation for the cartridge ε=0.95 and for the knife contact of the fuse link ε=0.4 [17]. It can be seen that with normal contact resistance, the highest temperature recorded by the thermovision camera is on the cartridge in the area of the fuse link, and with increased contact resistances, the highest temperature is on the contact knife.

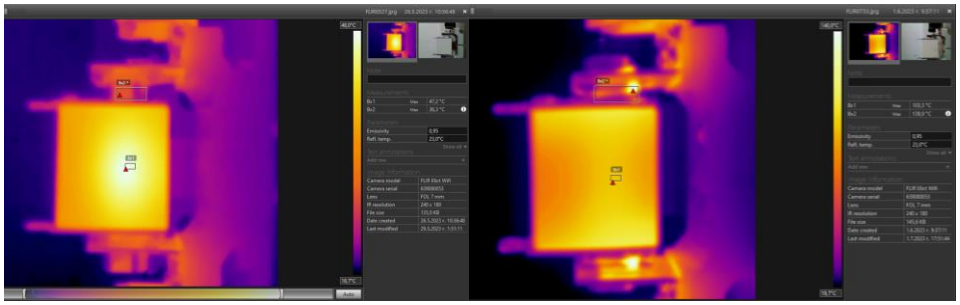

a) Normal contact resistances b) Increased contact resistances

Fig. 3 Thermovision fuse images at a time t=10 min and rated current of I_n=50 A

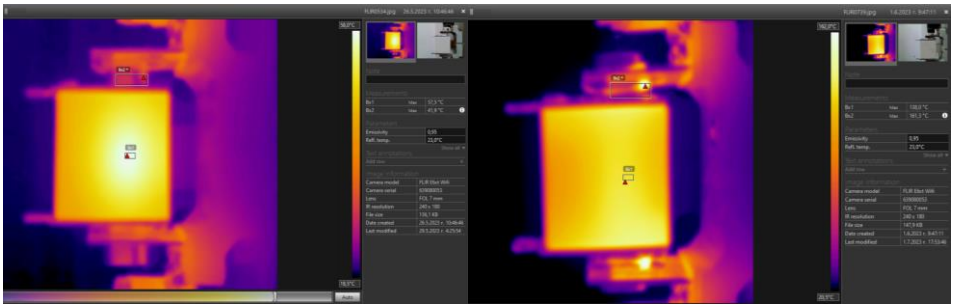

a) Normal contact resistances b) Increased contact resistances

Fig. 4 Thermovision fuse images at a time t=20 min and rated current of I_n=50 A

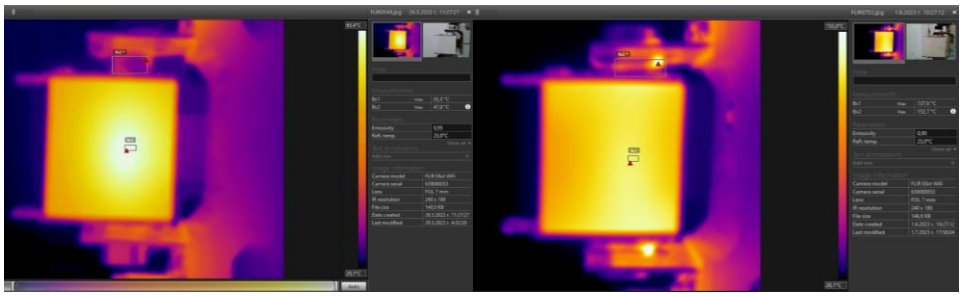

a) Normal contact resistances b) Increased contact resistances

Fig. 5 Thermovision fuse images at time t=60 min and rated current of I_n=50 A

Fig. 6 presents the graphical dependencies of the cartridge temperature and the temperature of the contact knife in a transient mode at normal and increased contact resistances, obtained by the thermovision camera. From the graphs it can be seen that the steady-state thermal mode of the fuse is reached in about 1 hour.

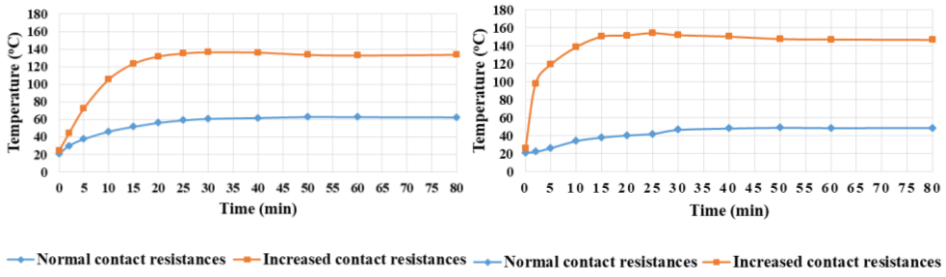

a) Cartridge b) Upper contact knife of the fuse

Fig. 6 Graphs of the cartridge heating in transient mode at rated current load of I_n=50 A for normal and increased contact resistances, obtained by using the thermovision method

3.3. Experimental results about the fuse heating at normal and increased resistances at a current load, higher than the rated current

After reaching steady-state thermal mode of the fuse, the values of the electric current within the range of the limit current were set and the actuation time of the fuse and its temperature at the moment of actuation were examined. Fig. 7 and Fig. 8 present thermovision images at fuse loads higher than the rated current load.

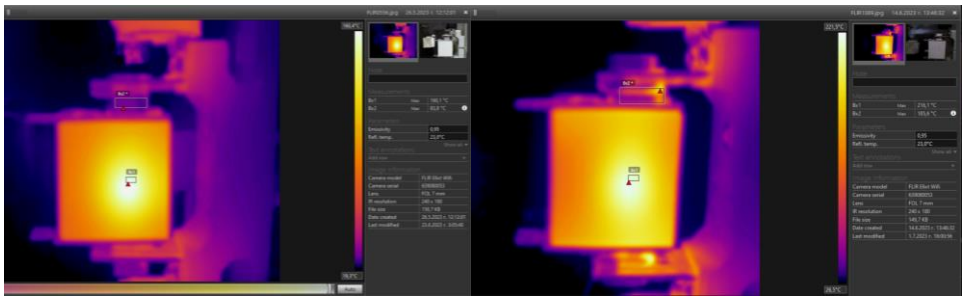

a) Normal contact resistances b) Increased contact resistances

Fig. 7 Thermovision fuse images at the moment of actuation at test current of I=80 A

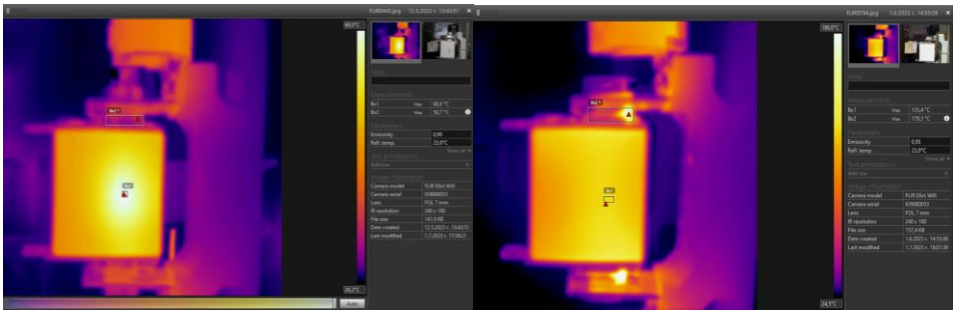

a) Normal contact resistances b) Increased contact resistances

Fig. 8 Thermovision fuse images at the moment of actuation at test current of I=150 A

Fig. 9 illustrates the dependence of the cartridge temperature, measured by means of a thermovision camera, on the test current both at normal and increased contact resistances. It can be seen that as the contact resistance increases, the fuse cartridge temperature also increases.

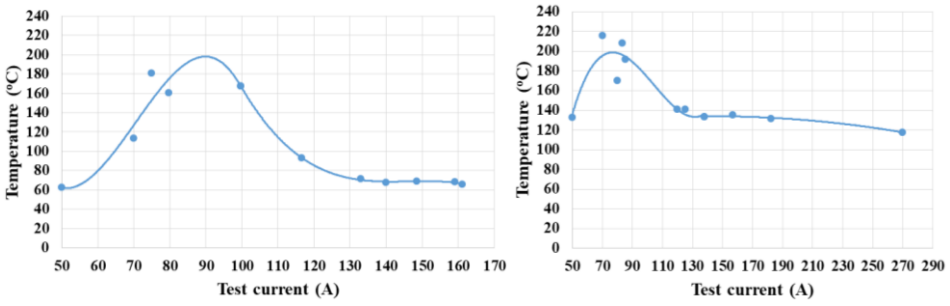

a) Normal contact resistances b) Increased contact resistances

Fig. 9 Cartridge heating at test current loads higher than the rated current

The time-current characteristics of the studied high-power low-voltage fuses at normal and increased contact resistances are shown in Fig. 10. At values of the electric current close to the limit current, as the contact resistance increases, losses in the contact connections increase, which leads to faster heating of the fuse link and hence to faster activation of the fuse.

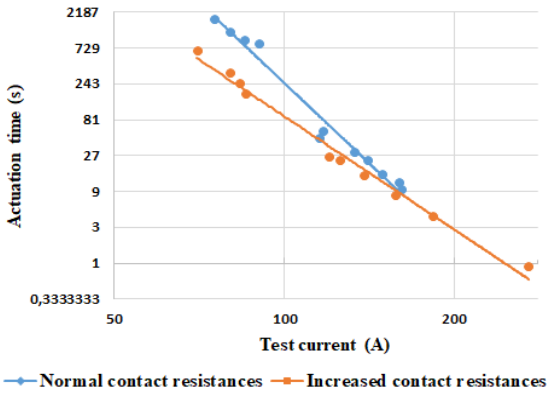

Fig. 10 Time-current characteristics at normal and increased contact resistances

4. Numerical Study of the High-Power Low-Voltage Fuse

4.1. Mathematical model

In order to build an adequate model, coupled electric field - thermal field problem has to be solved [18].

$$\nabla^2 V = 0,\ \boldsymbol{E} = -\nabla V,\ \boldsymbol{J} = \sigma(T)\cdot\boldsymbol{E},\ q = \sigma(T)\cdot\boldsymbol{E}^2, \tag{1}$$

where: V - electric scalar potential; $\boldsymbol{E}$ - vector of the electric field intensity; $\boldsymbol{J}$ - current density vector; q - heating power density; σ - electrical conductivity, which is equal to:

$$\sigma(T) = \frac{1}{\rho_o \cdot [1 + \alpha \cdot (T - T_o)]}, \tag{2}$$

where: ρ_o is the electrical resistivity at temperature T_o; T is the temperature of a volume of the conductive element; α is the thermal coefficient of the electrical resistivity.

This expression defines the specific surface losses in the contact connections:

$$p_c = \sigma_s \cdot \boldsymbol{E}^2, \tag{3}$$

where σ_s is the specific surface conductivity per unit area, defined by:

$$\sigma_s = \frac{1}{R_c \cdot S_c}, \tag{4}$$

where: R_c is an experimentally obtained value of the contact resistance; S_c is the apparent contact area according to Fig. 1. The values of the apparent contact areas for the contact knives are S_{c12}=S_{c13}=112 mm^2.

In order to solve the electric problem, the following boundary conditions are used:

- electric current I is set to the cross-section of the high-power fuse incoming conductor;
- electric potential of V=0 V is set to the cross-section of the high-power fuse outgoing conductor;
- the following boundary condition is imposed on the surface of the current-carrying elements:

$$\mathbf{n} \cdot \mathbf{J} = 0. \tag{5}$$

After the electric problem is solved, the power losses in the conductive elements of the high-power fuse, conductors and contact connections are obtained and used as heat sources for solving the thermal field problem.

In order to obtain the distribution of the thermal field in the high-power fuse, the thermal problem needs to be solved. The following equation describes it:

$$\gamma c \frac{\partial T}{\partial t} = \nabla.(\lambda \nabla T) + q \tag{6}$$

where: λ is the thermal conductivity; c is the specific heat; γ is the material volume density; T is the temperature in the considered point of the fuse; t is the time; q is the heating power density.

The thermal problem is solved at the following boundary conditions:

- heat transfer from the cartridge of the fuse toward the environment by convection and radiation:

$$-\lambda \cdot \left(\frac{\partial T}{\partial n} \right) = h \cdot (T_s - T_{amb}), \quad \lambda \cdot \left(\frac{\partial T}{\partial n} \right) = \varepsilon \cdot k \cdot (T_s^4 - T_{amb}^4), \tag{7}$$

where: h is a coefficient of convection, defined by the criterion of Nusselt in the program COMSOL; k is the constant of Stephan Boltzmann; ε is the emissivity; T_s is the temperature of the outer surface of the fuse; T_{amb} is the ambient temperature.

4.2. Finite element analysis

The numerical studies were conducted with the help of a developed 3D computer model in COMSOL [19]. The coupled problem electrtic field - thermal field in transient mode was solved. The finite element method was used to analyze the model and the resultant mesh is given in Fig. 11. The mesh consists of 548678 tetrahedral elements. An "extremely fine" mesh with a minimum element size of 0.225 mm was used. In areas with a large field gradient, the mesh is denser, and in areas with a small field gradient, the mesh is coarser.

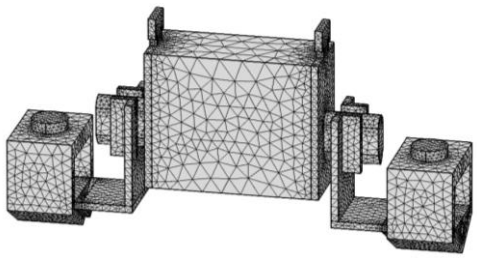

Fig. 11 Finite elements mesh

4.3. Numerical results about the fuse heating at normal and increased contact resistances at rated current load

The studies of the fuse heating were performed in a transient mode at different current loads and both with normal contact resistances R_{nc}=0.028 mΩ and at increased contact resistances R_{ic}=7.355 mΩ. Results were obtained about the influence of the contact resistance on the fuse heating, accordingly. Part of them is shown in Fig. 12÷17.

a) Normal contact resistances b) Increased contact resistances

Fig. 12 Distribution of the thermal field (°C) in fuse link at time t=10 min and rated current of I_n=50 A

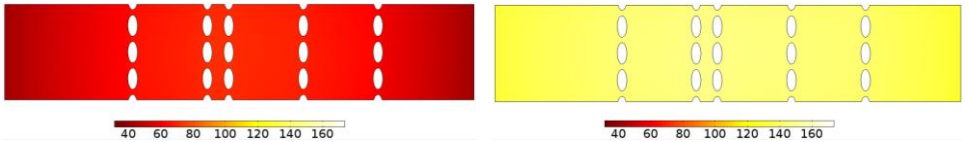

a) Normal contact resistances b) Increased contact resistances

Fig. 13 Distribution of the thermal field (°C) in fuse link at time t=20 min and rated current of I_n=50 A

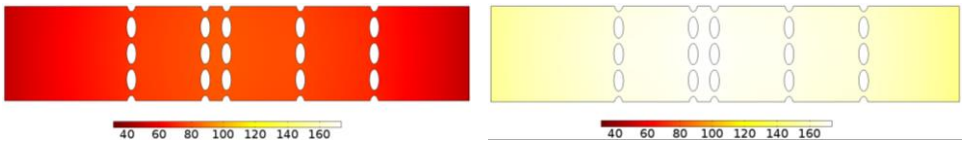

a) Normal contact resistances b) Increased contact resistances

Fig. 14 Distribution of the thermal field (°C) in fuse link at time t=60 min and rated current of I_n=50 A

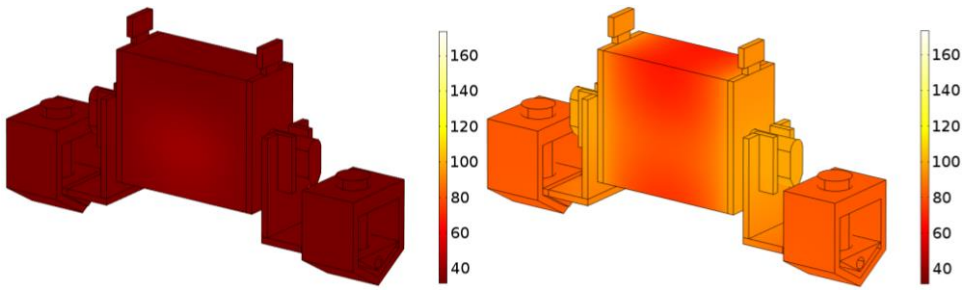

a) Normal contact resistances b) Increased contact resistances

Fig. 15 Distribution of the thermal field (°C) on the surface and on the base of the fuse at time t=10 min and rated current of I_n=50 A

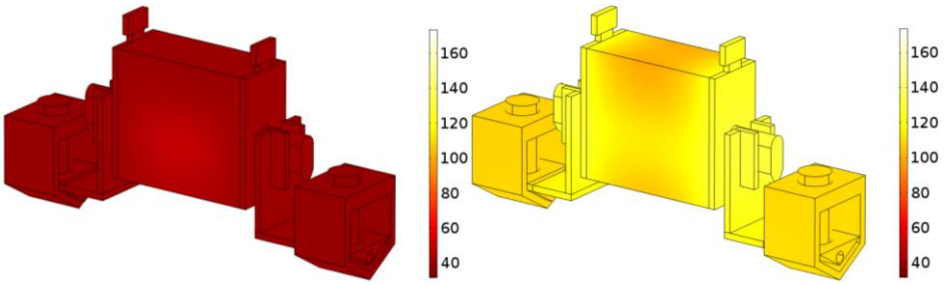

a) Normal contact resistances b) Increased contact resistances

Fig. 16 Distribution of the thermal field (°C) on the surface and on the base of the fuse at time t=20 min and rated current of I_n=50 A

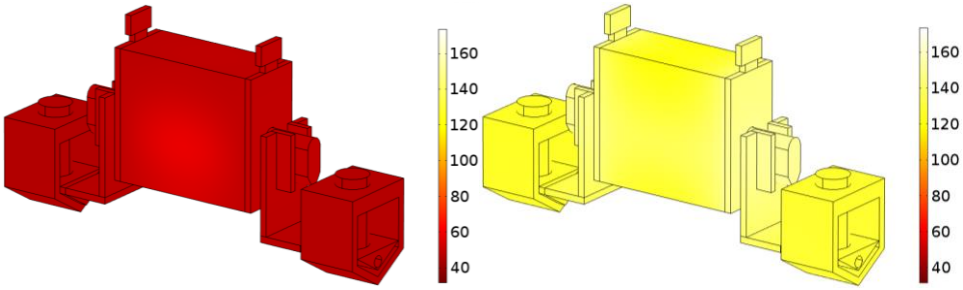

a) Normal contact resistances b) Increased contact resistances

Fig. 17 Distribution of the thermal field (°C) on the surface and on the base of the fuse at time t=60 min and rated current of I_n=50 A

Fig. 18 and Fig. 19 present comparisons between the obtained experimental and numerical results for a transient mode and normal or increased contact resistances at a rated current load of I_n=50 A.

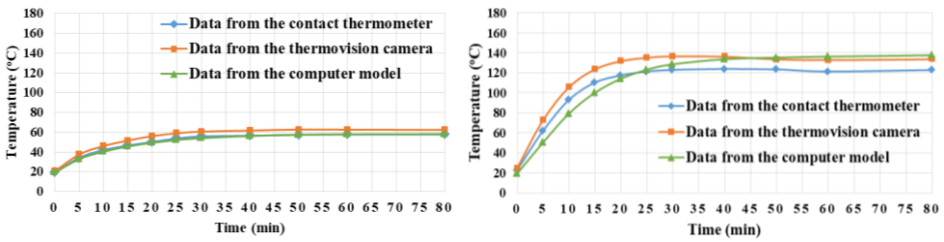

a) Normal contact resistances b) Increased contact resistances

Fig. 18 Comparison of the cartridge temperature in transient mode, obtained by the numerical model, the contact thermometer and the thermovision camera

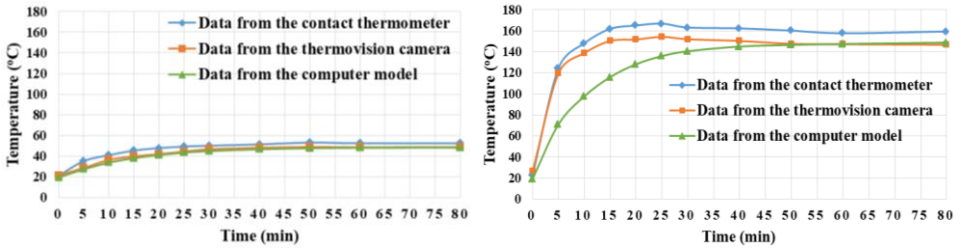

a) Normal contact resistances b) Increased contact resistances

Fig. 19 Comparison of the fuse contact knife temperature in transient mode, obtained by the numerical model, the contact thermometer and the thermovision camera

4.4. Numerical results about the fuse heating at normal and increased contact resistances and current load higher than the rated current

Studies on the fuse heating in a transient mode at current loads with values around the limit current were performed by means of a computer model. The transient thermal mode was modeled after reaching steady-state thermal mode at a rated current load. Studies were also conducted at normal contact resistances R_{nc}=0.028 mΩ and increased contact resistances R_{ic}=7.355 mΩ between the fuse contact knives and the fuse base. Numerical results about the influence of the contact resistance on the fuse heating were obtained. The conducted numerical studies concern the moment before the activation of the fuse, because the model does not reflect the processes of phase transition of the fuse link material from a solid to a liquid state. Part of these results is shown in Fig. 20÷23.

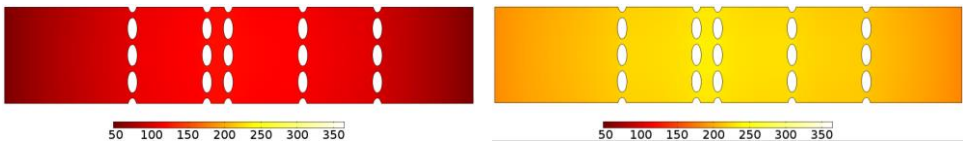

a) Normal contact resistances b) Increased contact resistances

Fig. 20 Distribution of the thermal field (°C) in the fuse link at time t=1 min and test current of I=75 A

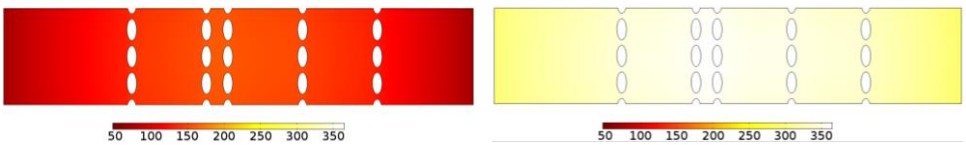

a) Normal contact resistances b) Increased contact resistances

Fig. 21 Distribution of the thermal field (°C) in the fuse link at time t=10 min and test current of I=75 A

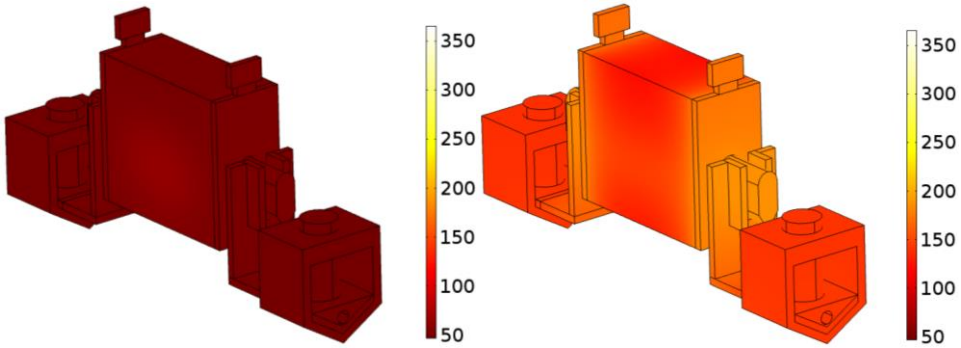

a) Normal contact resistances b) Increased contact resistances

Fig. 22 Distribution of the thermal field (°C) on the surface and on the base of the fuse at time t=1 min and test current of I_n=75 A

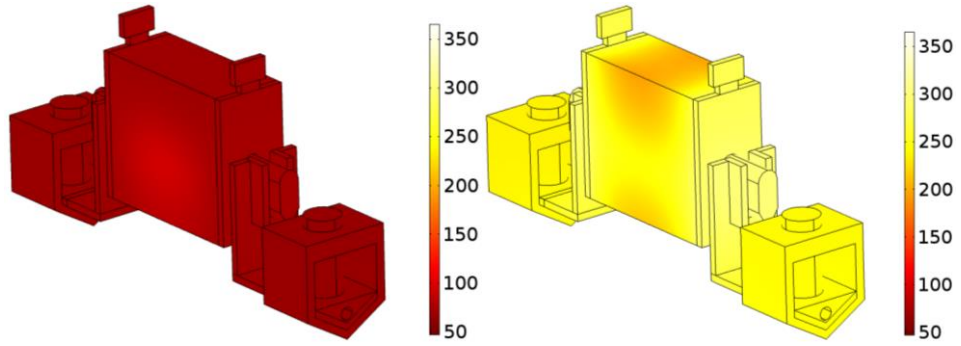

a) Normal contact resistances b) Increased contact resistances

Fig. 23 Distribution of the thermal field (°C) on the surface and on the base of the fuse at time t=10 min and test current of I=75 A

Fig. 24 makes comparisons between the obtained experimental and numerical results about the transient thermal mode at normal contact resistances and a test current of I=75 A.

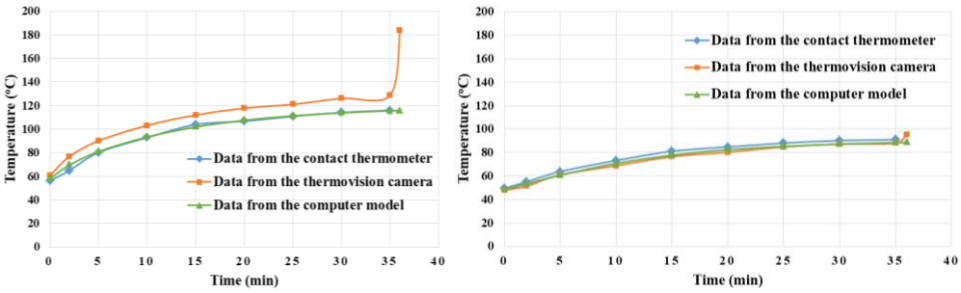

a) Cartridge b) Contact knife

Fig. 24 Comparison between the fuse temperature in transient mode at normal contact resistances and test current I=75 A, obtained by the numerical model, the contact thermometer, and the thermovision camera, correspondingly

Fig. 25 shows the change in the maximum value of the fuse link temperature in a transient mode, obtained by means of the computer model before the moment of fuse activation and at test current of I=75 A.

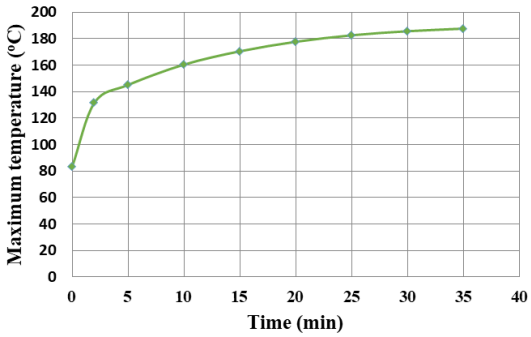

Fig. 25 Change in the maximum link temperature in transient thermal mode before the fuse activation at test current of I=75 A and normal contact resistances

5. CONCLUSION

The cartridge temperature, measured by a contact thermometer and obtained from a thermovision image differs by up to 10 %. The main factors, contributing to this difference, are the surface emissivity, as well as unidentified systematic influence of external infrared radiation. This error can be corrected by a correction factor. This confirms the applicability of the thermal imaging method for remote diagnosis and assessment of the state of fusible fuses during their operation.

The increased contact resistance of the knife contacts significantly influences on the limiting current of the studied fuses, including at overload currents of up to about 2.6 times higher than the rated current. Above these currents the influence of the increased contact resistance on the time for activation is insignificant. This can be explained by the fact that in this case, the thermal processes in the fuse, due to its big thermal capacity, begin to acquire an adiabatic character. This is also confirmed by the character of the cartridge temperature change due to the current, at fuse loading with currents, higher than the rated current.

At normal contact resistances, the results, obtained from the computer model up to the moment of fuse activation, differ from the experimental results, obtained by the contact thermometer, by up to 10% in transient mode and by up to 6% at steady-state mode. The bigger difference in the transient mode is due to the lack of real data on the values of the specific heat capacity of the materials of the studied fuse. At increased contact resistances in the transient mode, the difference between the obtained numerical and experimental results is greater than that at normal contact resistances. This is due to the change (instability) of the increased contact resistance during the transient process in result of the higher heating of the contact connection.

Fig. 24a illustrates that the cartridge temperature, measured by a thermovision camera at the moment of fuse activation, quickly goes up. This is due to the non-simultaneous interruption of the narrowed sections of the fuse link, as a result of which the power losses increase significantly. The metallurgical effect has an additional influence on this process. The

computer model does not take into account these processes. It is a matter of a future work to further develop the computer model with the aim of modeling the thermal processes during the phase transition of the link material from a solid to a liquid state.

REFERENCES

[1] I. Hadzhiev, D. Malamov, N. Kolev, I. Balabozov and I. Yatchev, "Study of the time-current characteristic of a high-power fuse in the limiting current region", In Proceedings of the 16th International Conference on Applied Electromagnetics - ΠΕС 2023, August 28-30, 2023, Niš, Serbia, pp.1–4.

[2] H. Farahani and M. Sabaghi, "Analysis of current harmonic on power system fuses using ANSYS", *Indian Journal of Science and Technology*, vol. 5, no. 3, 2012.

[3] R. Han, T. Wang, Q. Wang, Y. Zheng and L. Dong, "Analysis for fusing time of fuse under effect of harmonics based on fe method", In Proceedings of the 2016 China International Conference on Electricity Distribution (CICED 2016), Xi'an, China, 2016, pp. 1–5.

[4] A. Plesca, "Thermal analysis of the fuse with unequal links using finite element method", *International Journal of Electrical, Computer, Energetic, Electronic and Communication Engineering*, vol. 6, no. 12, 2012.

[5] M. Sarajlić, P. Kitak, M. Hribernik and J. Pihler, "Comparison between the measured and model-calculated temperature of the LV melting fuse", *WSEAS Transactions on Circuits and Systems*, vol. 18, 2019, pp. 63–66.

[6] P. Köllensperger, S. Böhm, M. Hilscher, P. Domanits and V. Seefeld, "Design and verification of a simulation model for fuses with high-breaking capacity", In Proceedings of the 2009 IEEE Energy Conversion Congress and Exposition, San Jose, USA, 2009, pp. 1261–1266.

[7] Y. Ishikawa, K. Hirose, M. Asayama, Y. Yamano and S. Kobayashi, "Dependence of current interruption performance on the element patterns of etched fuses", In Proceedings of the 2007 8th International Conference on Electric Fuses and their Applications, Ceyrat, France, 2007, pp. 51–56.

[8] A. Plesca, "A complete 3D thermal model for fast fuses", In Proceedings of the 2007 8th International Conference on Electric Fuses and their Applications, Ceyrat, France, 2007, pp. 79–85.

[9] R. Tzeneva, Y. Slavtchev and V. Mateev, "Modeling of thermal field of electrical fuses for domestic application", In Proceeding of Technical University of Sofia, vol. 64, no. 4, 2014, pp. 105–112.

[10] I. Hadzhiev, D. Malamov, I. Balabozov and I. Yatchev, "Experimental and numerical analysis of the thermal field in a high power low voltage fuse", In Proceedings of the 16th Conference on Electrical Machines, Drives and Power Systems (ELMA), Varna, Bulgaria, 2019, pp.1–5.

[11] I. Hadzhiev, D. Malamov, N. Kolev, I. Balabozov and I. Yatchev, "Thermal diagnostics of a high power fuse with thermovision camera", In Proceedings of the International Conference on Electrical, Computer, Communications and Mechatronics Engineering (ICECCME), Male, Maldives, 2022, pp.1–4.

[12] I. Hadzhiev, D. Malamov, I. Balabozov and I. Yatchev, "Analysis of the influence of some factors on the electric field and thermal field of a high power low voltage fuse", In Proceedings of the 14th International Conference on Applied Electromagnetics - ΠΕС 2019, Niš, Serbia, pp. 1–4.

[13] I. Hadzhiev, "Influence of the cables on the heating of a high power low voltage fuse", Youth Forums "Science, Technology, Innovation, Business - 2020", Plovdiv, Bulgaria, pp. 173–176.

[14] I. Hadzhiev, D. Malamov, I. Balabozov, I. Bayrev and I. Yatchev, "Numerical analysis of the influence of external losses on the heating of a high power fuse", 2023 International Aegean Conference on Electrical Machines and Power Electronics and 2023 International Conference on Optimization of Electrical and Electronic Equipment, ACEMP-OPTIM 2023, Istanbul, Turkey, pp. 1-8.

[15] I. Hadzhiev, D. Malamov, I. Balabozov and I. Yatchev, "Numerical analysis and experimental study of the thermal field in a power distribution block", 19th International Symposium on Electromagnetic Fields in Mechatronics, Electrical and Electronic Engineering, ISEF 2019, Nancy, France, pp. 1-2.

[16] EN 60269-1:2007 – Low-voltage fuses – Part 1: General requirements.

[17] J. H. Lienhard IV and J. H. Lienhard V, A heat transfer textbook 3th edition, Phlogiston Press, 2004.

[18] I. Yatchev and I. Marinova, Numerical methods and modeling of circuits and fields - part I, Sofia, 2011, (in Bulgarian).

[19] COMSOL Multiphysics 5.3 User's Guide, COMSOL Inc., 2018.